Since January 2020 Elsevier has created a COVID-19 resource centre with free information in English and Mandarin on the novel coronavirus COVID-19. The COVID-19 resource centre is hosted on Elsevier Connect, the company's public news and information website.

Veterinary Immunology and Immunopathology 145 (2012) 206–213

Contents lists available at SciVerse ScienceDirect

Veterinary Immunology and Immunopathology

journal homepage: www.elsevier.com/locate/vetimm

Research paper

Proteomic alteration of Marc-145 cells and PAMs after infection by porcine reproductive and respiratory syndrome virus

Zhuang Ding[a,1], Zhi-jie Li[b,1], Xiao-dong Zhang[a], Ya-gang Li[c], Chang-jun Liu[b], Yan-Ping Zhang[b], Yang Li[a,*]

[a] College of Animal Science and Veterinary Medicine, Key Laboratory of Zoonosis, Ministry of Education, Institute of Zoonosis, Jilin University, Changchun 130062, PR China
[b] Harbin Veterinary Research Institute, Chinese Academy of Agricultural Sciences, Harbin 150001, PR China
[c] Fourth Hospital of Jilin University, Changchun 130062, PR China

ARTICLE INFO

Article history:
Received 21 December 2010
Received in revised form 9 November 2011
Accepted 11 November 2011

Keywords:
Porcine reproductive and respiratory syndrome virus
Marc-145 cells
Cellular proteins
Proteomics

ABSTRACT

Viral infections usually result in alterations in the host cell proteome, which determine the fate of infected cells and the progress of pathogenesis. To uncover cellular protein responses in porcine reproductive and respiratory syndrome virus (PRRSV), infected pulmonary alveolar macrophages (PAMs) and Marc-145 cells were subjected to proteomic analysis involving two-dimensional electrophoresis (2-DE) followed by MALDI-TOF-MS/MS identification. Altered expression of 44 protein spots in infected cells was identified in 2D gels, of which the 29 characterised by MALDI-TOF-MS/MS included 17 up-regulated and 12 down-regulated proteins. Some of these proteins were further confirmed at the mRNA level using real-time RT-PCR. Moreover, Western blot analysis confirmed the up-regulation of HSP27, vimentin and the down-regulation of galectin-1. Our study is the first attempt to analyze the cellular protein profile of PRRSV-infected Marc-145 cells using proteomics to provide valuable information about the effects of PRRSV-induced alterations on Marc-145 cell function. Further study of the affected proteins may facilitate our understanding of the mechanisms of PRRSV infection and pathogenesis.

1. Introduction

Porcine reproductive and respiratory syndrome (PRRS) is one of the most economically significant viral diseases of swine and a frustrating challenge to the global swine industry. It is characterised by severe reproductive failure in sows and respiratory distress in growing pigs and piglets (Wensvoort et al., 1992). Porcine reproductive and respiratory syndrome virus (PRRSV), the causative agent of PRRS, is a member of the Arteriviridae family. This family is composed of a group of positive (+) sense, single-stranded RNA viruses including simian hemorrhagic fever virus (SHFV), equine arteritis virus (EAV), and lactate dehydrogenase-elevating virus (LDV). PRRSV has a highly restricted cell tropism, both in vivo and in vitro (Kim et al., 1993). The virus infects the African green monkey kidney cell line MA-104 and its derivatives, Marc-145 and CL-2621, in vitro. PRRSV preferentially infects cells of the monocyte/macrophage lineage, especially porcine alveolar macrophages (PAMs), in the natural host (Duan et al., 1997). In both PAMs and monkey kidney-derived cell lines, the virus enters through a mechanism of receptor-mediated endocytosis (Nauwynck et al., 1999).

Little is known about the molecular mechanisms of PRRSV pathogenesis. Complex and mutual virus–host cell interactions occur when a virus invades the host. However, most of the cellular functions affected by PRRSV infection are still unidentified; hence, a comprehensive study of the interactions between PRRSV and PRRSV-infected host cells was necessary.

* Corresponding author. Tel.: +86 431 87836401.
E-mail address: myth0318@yahoo.cn (Y. Li).
[1] Contributed equally to this work.

0165-2427/$ – see front matter © 2011 Elsevier B.V. All rights reserved.
doi:10.1016/j.vetimm.2011.11.005

Proteomic analysis of host cellular responses to virus infection may provide new insight into cellular mechanisms involved in viral pathogenesis. To date, proteomic approaches, e.g., coupling two-dimensional electrophoresis (2-DE) and mass spectrometry (MS) (Blackstock and Weir, 1999), have been widely used to study mechanisms of viral infection through the comparative analysis of cellular protein profiles (Alfonso et al., 2004; Zheng et al., 2008; Ringrose et al., 2008). This procedure of comparing protein expression patterns of normal and infected cells can provide exclusive information about the response of host cells to viral infection. Proteomic changes in infected host cells have been studied for many pathogenic mammalian viruses, including human immunodeficiency virus type-1 (HIV-1), severe acute respiratory syndrome (SARS)-associated coronavirus, rabies virus, Nipah virus and African swine fever virus. The purpose of this paper is to analyze the changes in cellular proteins of Marc-145 cells and PAMs exposed to PRRSV. Furthermore, we also discuss the altered functions of Marc-145 cells and PAMs, induced by PRRSV infection.

2. Materials and methods

2.1. Virus and cell culture

PRRSV JL/07/SW used for this study was isolated from an intensive pig farm with a typical PRRS outbreak in Jilin province of China in 2007. A stock of the virus was the fifth passage cell culture prepared in Marc-145 cells with a titer of $10^{6.19}$ $TCID_{50}$/mL. Marc-145 cells were grown in Dulbecco's modified Eagle's medium (DMEM; Invitrogen) supplemented with 10% fetal bovine serum (FBS; Invitrogen), 100 U/mL Penicillin G, 100 mg/mL Na streptomycin sulfate, and 2 mM L-glutamine. Pulmonary alveolar macrophages (PAMs) were prepared using lung lavage technique as previously described (Wensvoort et al., 1991) with minor modifications from three 6-week-old specific-pathogen-free (SPF) piglets (Beijing Center for SPF Swine Breeding and Management) that were free of PRRSV, porcine parvovirus, pseudorabies virus, swine influenza virus and *Mycoplasma hyopneumoniae* infections.

2.2. Virus inoculation

PAMs were incubated for 12 h at 37 °C in 5% CO_2 in RPMI-1640 medium, and the nonadherent cells were moved by gentle washing with RPMI-1640 medium before inoculation. Then, the cells (PAMs and Marc-145 cells) were inoculated with the virulent PRRSV strain JL/07/SW at an input multiplicity of about 2 $TCID_{50}$/cell. The uninfected cells served as mock-infected cells. Viral propagation was confirmed by daily observation of the cytopathic effect (CPE) and indirect immunofluorescence assay. After 12, 24, 36, 48, 60 and 72 h, the infection rate was monitored by indirect fluorescent-antibody (IFA) staining of cells, numbers of infected cells were quantitated by fluorescence microscopy.

2.3. Extraction of cellular proteins

The collected cells were lysed with lysis buffer (8 M urea, 2 M thiourea, 4% CHAPS, 40 mM Tris, 0.5% IPG buffer) containing complete protease inhibitor cocktail tablets (Roche). Approximate 5×10^7 cells were lysed in 1 mL lysis buffer. After vortex vigorously, the solution was centrifuged at 20 000 × *g* for 1 h at 4 °C. Uninfected cells were treated in parallel in the same way. The protein concentration was determined by the Coomassie Plus—The Better Bradford Assay Kit (Pierce Biotechnology, Rockford). The clear supernatants were collected and stored at −80 °C until use to prevent protein degradation. Three flasks of uninfected cells, as controls, were treated in parallel in the same way.

2.4. Two-dimensional gel electrophoresis

Approximately 300 μg proteins were loaded for first-dimensional separation. The samples were analyzed by 2-DE using commercial IPG strips (pH 4–7, 18 cm) (GE Healthcare) for IEF and standard vertical SDS-PAGE (12% acrylamide:bisacrylamide) for second dimension. IPG strips were rehydrated in a rehydration buffer consisting of 7 M urea, 2 M thiourea, 2% CHAPS, 65 mM DTT and 0.5% IPG buffer 4–7 for 13 h at room temperature with passive rehydration. Focusing was carried out at 20 °C with the current limited to 50 μA/strip using IPGPhor II (GE Healthcare). The program was performed as follows: 100 V for 1.5 h, 250 V for 0.5 h, 500 V for 1 h, 1000 V for 1 h, 3000 V for 1 h, 5000 V for 1 h, gradient ramping to 8000 V for 3 h, then 8000 V for a total of 60 000 Vh. Prior to the second dimension, IPG strips were equilibrated for 15 min with gentle shaking in equilibration solution I containing 6 M urea, 2% (w/v) sodium dodecyl sulfate (SDS), 30% (v/v) glycerol, 50 mM Tris–HCl (pH 8.8), reduced with 2% (w/v) DTT and a trace of bromophenol blue. After equilibration, proteins were separated on second-dimension separation, at a constant current of 1 w/gel for 30 min, then 10 w/gel until the dye reached the bottom of the gel. The strips were sealed on the top of the gels using a sealing solution (1% agarose, 0.5% SDS, 0.5 M Tris–HCl). The run was completed once the bromophenol blue reached the bottom or run of the gel. During the whole run, the temperature was set at 16 °C. Three independent cell cultures were conducted for biological replicates.

2.5. Gel staining and image analysis

The gels were stained by the modified silver staining method compatible with MS (Yan et al., 2000). The stained gels were scanned in an Image Scanner operated by LabScan 3.00 software. Image analysis was carried out with Image-Master 2D Platinum 6.0 according to manufacturer's protocol (GE Healthcare). At least three replicates from independent cultures were done for each point and data were analyzed by Student's *t*-test. Only the significantly differentially expressed protein spots ($p < 0.05$) with 1.5-fold different intensity or more were selected and subjected to identification by MS.

2.6. In-gel digestion

The protein spots were manually excised from the silver-stained gels and then transferred to V-bottom 96-well microplates loaded with 100 μL of 50% ACN, 25 mM ammonium bicarbonate solution/well. After being destained for 1 h, gel plugs were dehydrated with 100 μL of 100% ACN for 20 min and then thoroughly dried in a SpeedVac concentrator (Thermo Savant, U.S.A.) for 30 min. The dried gel particles were rehydrated at 4 °C for 45 min with 2 μL/well trypsin (Promega, Madison, WI) in 25 mM ammonium bicarbonate and then incubated at 37 °C for 12 h. After trypsin digestion, the peptide mixtures were extracted with 8 μL of extraction solution (50% ACN, 0.5% TFA)/well at 37 °C for 1 h. Finally the extracts were dried under the protection of N2.

2.7. MALDI-TOF/TOF MS and MS/MS analysis and database search

The peptide mixtures were redissolved in 0.8 μL of matrix solution (α-cyano-4-hydroxycinnamic acid (Sigma) in 0.1% TFA, 50% ACN) and then loaded on the target plate. Samples were allowed to air dry at room temperature and analyzed by a 4700 MALDI-TOF/TOF Proteomics Analyzer (Applied Biosystems, Foster City, CA) with 355 nm Nd:YAG laser and 20 kV accelerated voltage. Trypsin-digested peptides of myoglobin were added to the six calibration spots on the MALDI plate to calibrate the mass instrument with internal calibration mode. All acquired spectra of samples were processed using 4700 Explore™ software (Applied Biosystems) in a default mode. Parent mass peaks with mass range of 700–3200 Da and minimum signal to noise ratio of 20 were picked out for tandem TOF/TOF analysis. Combined MS and MS/MS spectra were submitted to MASCOT (Version 2.1, Matrix Science, London, UK) by GPS Explorer software (Version 3.6, Applied Biosystems) and searched with the following parameters: National Center for Biotechnology Information non-redundant (NCBInr) database (release date, March 18, 2006), taxonomy of bony vertebrates or viruses, trypsin digest with one missing cleavage, no fixed modifications, MS tolerance of 0.2 Da, MS/MS tolerance of 0.6 Da, and possible oxidation of methionine.

2.8. Real-time RT-PCR

Total RNA was extracted from the samples using TRIzol (Invitrogen), according to the manufacturer's protocols. Two micrograms of total RNA was reverse transcribed with 200 U M-MLV Reverse Transcriptase (Invitrogen) and 500 ng Oligo(dT)18 as the first strand primer in 20 μL reaction solution. Specific primers were designed according to the corresponding gene sequences of MS-identified proteins using Beacon Designer software 7.5 (Primer Biosoft International). All the information on the primers is listed in Table 1. The real-time RT-PCR assays were performed using the iCycler® real-time PCR detection system (Bio-Rad Laboratory). Each 25 μL reaction volume contained 1 μL 10 μM (each) forward and reverse primers, 12.5 μL 2× SYBR® Premix Ex Taq™ II (Takara), and 2 μL 1:10 diluted cDNA products. The following PCR program was used for amplification: 30 s at 94 °C, 40 cycles of denaturation at 95 °C for 15 s, and annealing and extension at 55 °C for 30 s. All samples were analyzed in triplicate, and the average value of the triplicates was used for quantification. Quantitative analysis of the data was performed using the iCycler IQ5 optical system software version 2.0 (Bio-Rad Laboratory) in a normalized expression (ΔΔCT) model, using the mock-infected group as a calibrator (relative expression = 1) and GAPDH was used as an internal control.

2.9. Western blot analysis

The samples (20 μg) were separated by electrophoresis on 12% (w/v) SDS-PAGE. The fractionated proteins were transferred to PVDF membranes (Millipore, Bedford, MA) and blocked with TBS-T containing 5% BSA at 4 °C overnight. Primary antibodies used were goat anti-HSP27 polyclonal antibody (diluted 1:200, Santa Cruz, CA), goat anti-vimentin polyclonal antibody (diluted 1:100, Abcam, UK), rabbit anti-galectin-1 polyclonal antibody (diluted 1:1000, Abcam, UK) and mouse anti-β-actin antibody (diluted 1:1000, Santa Cruz Biotechnology, USA). The membranes were then incubated with the primary antibodies overnight at 4 °C. Immunoreactive protein bands were visualized with a chemiluminescence subtraction using SuperSignal West Pico chemiluminescence substrate (Pierce Biotechnology, Inc., Rockford, IL).

3. Result

3.1. Confirmation of PRRSV propagation in Marc-145 cells by IFA

Specific immuno fluorescence in Marc-145 cells and PAMs infected with PRRSV JL/07/SW was observed at 12, 24, 36, 48, 60 and 72 h post-inoculation (p.i.), but not in mock-infected cells. Meanwhile, CPE typical of PRRSV in Marc-145 cells and PAMs was seen at 36 h p.i. and 24 h p.i., respectively (data not shown). Mark-145 cells at 36 h p.i. and PAMs at 24 h p.i. were therefore selected for proteomic analysis.

3.2. Two-dimensional gel electrophoresis profiles of PRRSV-infected Marc-145 cells and PAMs

The cellular proteins in mock-infected cells and PRRSV-infected Marc-145 cells and PAMs were extracted for 2-DE analysis. To compensate for the variability of gel electrophoresis, three independent 2-DE gels of cellular extracts from mock-infected or PRRSV-infected Marc-145 cells and PAMs were selected for statistical analysis. A pH gradient of 4–7 was determined to be optimum for the separation of Marc-145 and PAM proteins. A total of 44 protein spots were differentially expressed in PRRSV-infected cells as compared to mock-infected cells (Fig. 1), including 23 significantly up-regulated and 21 significantly down-regulated protein spots on 2D gels.

Table 1
Primers used for real-time RT-PCR.

Gene symbol	Gene accession number	Forward primer sequence (5′-3′)	Reverse primer sequence (5′-3′)	Amplicon size (bp)
Pulmonary alveolar macrophages (PAMs)				
HSPB1	NM_001007518	CAGCAGCGGCGTCTCGGAG	GCCGCTCCTCGTGCTTGCCCGTG	140
Vimentin	AY368193	ATTGAGATTGCCACCTACAGG	ATGAGATAATGCATAGAAAGCG	126
Galectin-1	AY604429	TCGCCAGCAACCTGAATCTCAAACC	GAGGGTTGAAGTGCAGGCACAGG	128
SOD1	GU944822	TTGGAGATAATACACAAGGCTG	CCAGGTCTCCAACGTGCCTC	105
GAPDH	NM_001206359	CAACGGATTTGGTCGTATTGGGCG	GGAATCATACTGGAACATGTAAACC	130
Marc-145 cell				
HSPB1	XM_001109274	CGGCAAGCACGAGGAGCGGCAGG	GGCTTCCACGGTCAGTGTGCCC	139
Peroxiredoxin-6	XM_001101473	CGGCAAGCACGAGGAGCGGCAGG	CTTCCACGGTCAGTGTGCCCTC	137
Galectin-1	NM_001168627	GCCAGCAACCTGAATCTCAAACC	GCCGTGGGCGTTGAAGCGAGGG	144
GAPDH	NM_001195426	AGGTGAAGGTCGGAGTCAACGG	ATGGGTGGAATCATACTGGAAC	152

3.3. Identification and functional classification of the differentially expressed proteins

To identify these differentially expressed cellular protein spots, the 44 protein spots were picked out of the stained gels, subjected to in-gel tryptic digestion and subsequent MALDI-TOF/TOF MS and MS/MS identification. Subjecting the combined MS and MS/MS analysis to a MASCOT scan of the NCBInr database successfully identified 29 proteins, including 17 up-regulated and 12 down-regulated proteins. A complete list of all proteins identified during PRRSV infection, their protein score and sequence

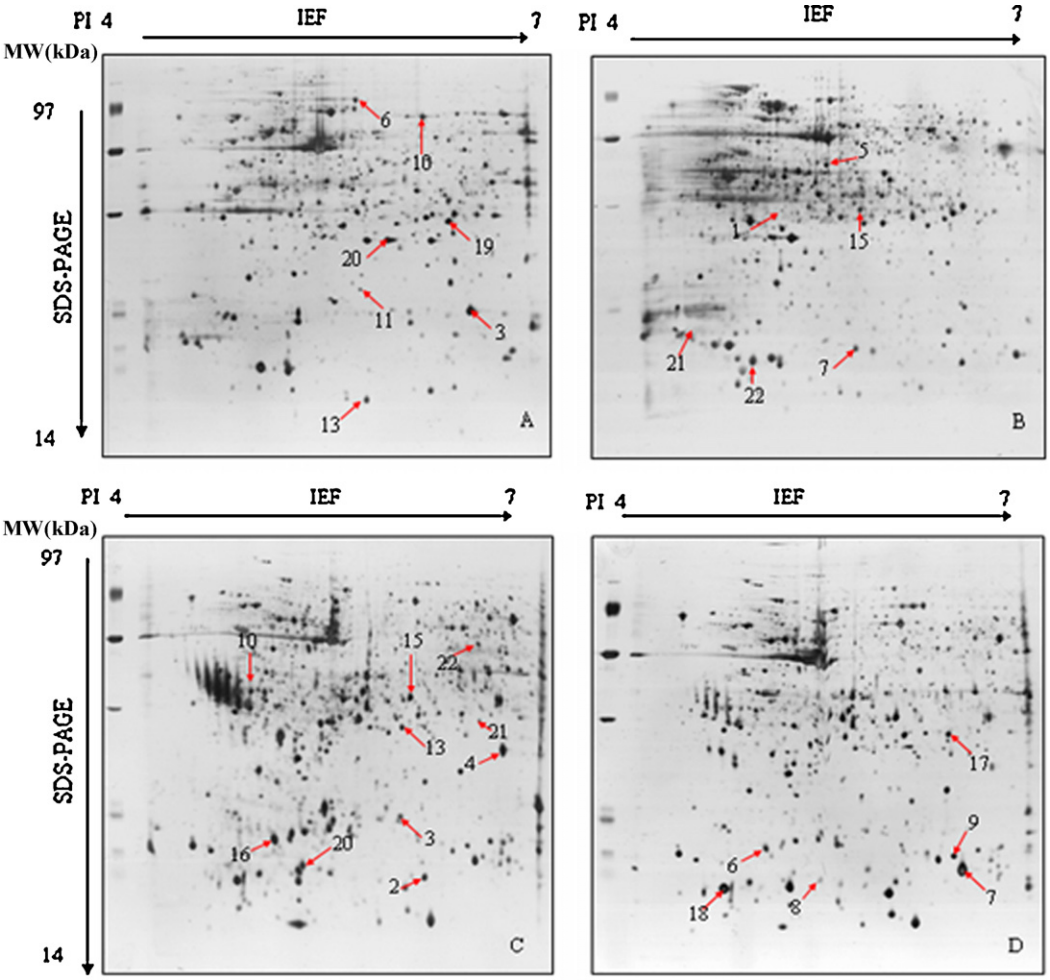

Fig. 1. 2-DE analysis of PRRSV-infected Marc-145 cells (A) and PAMs (C), mock-infected Marc-145 cells (B) and PAMs (D). Arrows indicate the isolated and identified protein spots with at least 1.5-fold up-regulation (A and C) or down-regulation (B and D). Spots are numbered according to Table 2. Equal amounts of total protein from infected and uninfected whole cell lysates were resolved by 2-D PAGE. The protein spots were visualized by silver staining.

Table 2
Identification of differentially expressed cellular proteins in PRRSV-infected Marc-145 cells and PAMs.

Spot number[a]	Protein name	Accession number[b]	MW (Da)	pI	Protein score	Sequence coverage (%)
Significantly up-regulated proteins						
Cytoskeletal protein						
M3	Cofilin-1	gi|73960624	25,773	6.93	248	82
P3	Actin-related protein	gi|62510460	16,278.3	5.47	127	50
P15	Vimentin	gi|418884	30,826.5	6.47	58	40
P16	Alpha-cardiac actin	gi|553859	16,758.2	5.29	128	30
P20	Cofilin-1	gi|51592135	18,506.6	8.16	156	18
Response to stress/anti-oxidative stress proteins						
M6	Stress-70 protein	gi|73970890	55,119.2	5.12	94	14
M11	Peroxiredoxin-2	gi|55727787	19,418	5.38	266	38
M20	Heat shock 27 kDa protein 1	gi|55926209	22,927.7	6.23	177	28
M19	Peroxiredoxin-6	gi|84579335	24,995.1	5.74	184	51
P13	Heat shock protein beta-1 (HSPB1)	gi|4504517	22,768.5	5.98	190	42
Ubiquitin–proteosome pathway						
M13	Ubiquitin	gi|51701919	8559.6	6.56	152	
Metabolic process						
P2	Cystatin-B (CSTB)	gi|76608397	25,288.5	6.44	97	31
P4	FYVE finger-containing phosphoinositide kinase	gi|6685475	232,904.3	6.34	77	20
P22	Pyruvate kinase isozymes M1/M2 (Pkm 2)	gi|206205	57,744	7.15	279	40
Others						
M10	UPF 0681 protein KIAA1033	gi|85397087	136,330.2	7.1	71	21
P10	Tropomyosin alpha-4 chain (TPM4)	gi|4507651	28,504.5	4.67	288	60
P21	UPF 0568 protein	gi|78369460	28,191.7	6.19	111	35
Significantly down-regulated proteins						
Cytoskeletal protein						
M5	LIM and SH3 protein 1	gi|6754508	29,975.3	6.61	97	41
M7	Plectin-1	gi|73974726	532,578.5	5.72	75	8
M21	Glial fibrillary acidic protein	gi|14193690	46,497.7	5.05	60	35
P6	Plectin-1	gi|73974724	516,572.1	5.6	111	24
Signaling transduction						
M22	Galectin-1	gi|84027796	14,736.2	5.65	78	10
P18	Galectin-1	gi|47716872	14,590.2	5.07	149	34
Response to stress/anti-oxidative stress proteins						
P9	Superoxide dismutase 1 (SOD1)	gi|15082144	15,236.6	6.04	201	61
Metabolic process						
M1	Prohibitin	gi|67970515	29,757.9	5.57	365	56
M15	Prohibitin	gi|67970515	29,757.9	5.57	365	56
P7	Epidermal fatty acid-binding protein 5 (Fabp5)	gi|89886167	15,199.5	6.6	128	30
P8	A-kinase anchoring protein AKAP350	gi|4558862	416,855.1	4.94	85	18
P17	Pyridoxine 5′-phosphate oxidase variant	gi|62898045	29,896.8	7.01	137	16

P: protein of porcine alveolar macrophages (PAMs). M: protein of Marc-145 cells.
[a] Refers to the labels of protein spots in Fig. 1.
[b] Accession number that was obtained through the input of MALDI-TOF MS/MS experimental results in a MASCOT search of the NCBInr database.

coverage are shown in Table 2. To better understand the implications of cellular responses to PRRSV infection, these proteins and their corresponding biological processes were categorised according to the UniProt Knowledgebase and Gene Ontology Database. The identified cellular proteins were mainly involved in morphogenesis, protein synthesis, metabolism, stress response, the ubiquitin–proteasome pathway (UPP) and signal transduction.

3.4. Analysis of identified proteins at the transcriptional level

Alterations in expression of a protein may be attributed to changes in its mRNA levels. To compare the results of the proteomics analysis to the corresponding mRNA levels, the transcriptional alterations in four selected proteins from PAMs and three selected proteins from Marc-145 cells were measured by real-time RT-PCR (Fig. 2). In PAMs, the mRNA level of HSP27 and vimentin was increased by 1.22- and 1.56-fold, respectively, and the trends of the changes in their mRNA levels were similar to the patterns of change in their corresponding proteins on 2-DE gels. For Marc-145 cells, the altered mRNA levels of HSPB1, peroxiredoxin-6 and galectin-1 were consistent with the 2-DE results. Interestingly, SOD1 mRNA levels displayed no obvious difference between PRRSV-infected and mock-infected cells.

3.5. Confirmation of proteomic data by Western blot analysis

To further confirm the alterations in protein expression during PRRSV infection, the following proteins were selected for Western blot analysis: HSP27 (up-regulated Marc-145 cellular protein), vimentin (up-regulated PAMs cellular protein) and galectin-1 (down-regulated in Marc-145 cells and PAMs). Fig. 3 shows an increase in the expression of vimentin and HSP27, and a decrease in the expression of galectin-1 during PRRSV infection, with no alterations in actin expression; hence, Western blotting results are consistent with those observed with 2D PAGE.

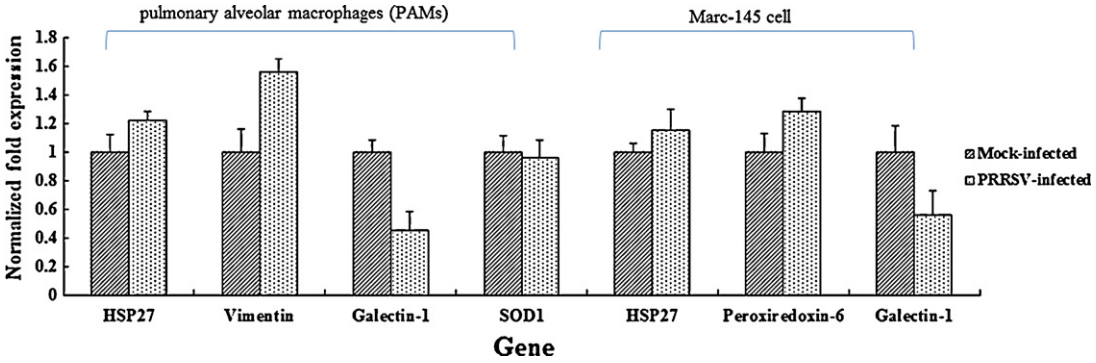

Fig. 2. Transcript alteration of seven selected genes in PAMs and Marc-145 cells from the PRRSV-infected group compared with the mock-infected group. Total RNA extracted from PAMs or Marc-145 cells was measured by real-time RT-PCR analysis; relative expression levels were calculated according to the $2^{-\Delta\Delta CT}$ method, using GAPDH as an internal reference gene and the mock-infected group as a calibrator (relative expression = 1). Error bars represent the standard deviation. For identification of gene symbols representing different genes, refer to Table 2.

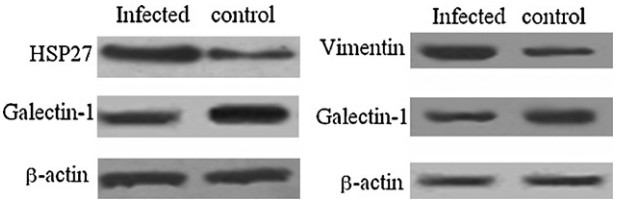

Fig. 3. Western blot confirmation of representative proteins in PRRSV-infected Marc-145 cells (A) and PAMs (B). Aliquots of 50 μg of protein extracts were loaded per lane and resolved by 12% SDS-PAGE gel. Western blot analysis was then performed using antibodies to the proteins of HSP27, vimentin, galectin-1 and β-actin. The latter was used as an internal control to normalize the quantitative data.

4. Discussion

Virus infection and the corresponding host response involve a complex interplay of host and viral networks in which many viruses attempt to subvert host cell processes to increase the efficiency of viral infection. Likewise, the host employs a number of responses to generate an anti-viral state (Emmott et al., 2010). Infection by different viruses causes alterations in the transcription and translation patterns of the host. Increasing evidence emphasises the use of comparative proteomics to screen the differentially expressed proteins associated with pathophysiological host cellular responses to viral infection. Understanding the changes in the cellular proteins of these cells after exposure to PRRSV could reveal molecular mechanisms associated with altered functions of PRRSV-infected Marc-145 cells and PAMs. In this study, proteomic methods coupled with real-time RT-PCR and Western blotting were applied to identify differentially expressed proteins in PRRSV-infected and mock-infected PAMs and Marc-145 cells. We now attempt to interpret the possible functional roles of some of the proteins identified during PRRSV infection.

In our study, one of the major findings was the increased levels of some cytoskeletal proteins, including cofilin-1 and vimentin, in the PRRSV-infected group. Although these proteins may not be specific to PRRSV, most cytoskeleton changes detected in PRRSV-infected cells were caused by PRRSV infection. Vimentin is an important cellular cytoskeleton component. Studies have reported a reorganisation of vimentin in certain viral infections, which probably leads to unstable cytoskeletal structure (Stefanovic et al., 2005). Differential proteomes of chicken embryo fibroblasts (CEFs), with and without IBDV infection, also showed considerable up- or down-regulation of many cytoskeletal proteins; the intermediate filament (IF) vimentin levels also significantly decreased (Zheng et al., 2008). Furthermore, Fatemel group reported that vimentin was up-regulated in CVS-infected BHK-21 cells (Zandi et al., 2009). In the present study, a decrease in the abundance of the actin-binding protein, plectin-1, in the PRRSV-infected group suggests that PRRSV may also manipulate the host cytoskeletal network for its own infectious processes and replication.

We identified another group of up-regulated proteins of interest in the ubiquitin–proteasome pathway, a major intracellular protein degradation pathway, which has recently been implicated in viral infections, including avoidance of host immune surveillance, viral maturation, viral progeny release, efficient viral replication, and reactivation of virus from latency (Gao and Luo, 2006). In this study, ubiquitin was identified as a differentially expressed cellular protein during PRRSV infection in Marc-145 cell. The best known function of ubiquitin in proteolysis is to serve as a signal for the target protein to be recognised and degraded by the proteasome. Although the host has a variety of defences to protect against viral infections, sometimes the immune response to the infection is the direct cause of tissue injury. Whether PRRSV takes the similar or different strategy during infection has not been elucidated and deserves further investigation.

Remarkably, several stress response and anti-oxidative proteins were significantly altered in the present study. HSPB1 is an important, small heat shock protein (HSP) that is synthesised in response to a wide variety of stressful stimuli, including viral infection. The abundance of HSPB1 increased in cells infected in vitro with H9N2 avian influenza virus (Liu et al., 2008), African swine fever virus (Alfonso et al., 2004), and infectious bursal disease virus (Zheng et al., 2008). In contrast, decreased levels

of HSPB1 were observed in cells infected in vitro with mumps virus (Yokota et al., 2003) and porcine circovirus type 2 (Zhang et al., 2009a,b), which suggest that HSPB1 may play different roles in different viral infections or different stages of infection. Two antioxidative stress proteins, peroxiredoxin-6 (Prx6) and peroxiredoxin-2 (Prx2), were up-regulated, suggesting that PRRSV infection may induce host cell oxidative stress. The cytosolic Prx2 has two highly conserved cysteine residues that become oxidised by hydrogen peroxide (H_2O_2) and hydroperoxides, resulting in the reversible formation of a homodimer (Wood et al., 2003). Human erythrocyte Prx2 reacts extremely rapidly with H_2O_2, with a rate constant similar to those observed for catalases and glutathione peroxidases. Prx6 is a bifunctional 25 kDa protein with both GSH (glutathione) peroxidase and phospholipase A2 activities. Overexpression of Prx6 in cells can protect against oxidative stress, whereas antisense treatment results in oxidative stress and apoptosis (Manevich and Fisher, 2005). We report an increase in the abundance of HSP27 and Prx6 after PRRSV infection in Marc-145 cells and PAMs as measured by 2-DE and real-time RT-PCR. Furthermore, the change in HSP27 expression was confirmed by Western blotting. This alteration may allow infected cells to be eliminated by apoptosis, or serve as a form of host defence against PRRSV infection.

Virus-induced oxidative stress is associated with the activation of phagocytosis and the release of reactive oxygen species (ROS), which play a positive modulatory role in immune activation, eradication of viral infection and immune-induced cellular injury (Schwarz, 1996). Superoxide dismutase 1 (SOD1) is localised in both the cytoplasm and intermembrane space of mitochondria. Because of its ability to scavenge superoxide, SOD1 is considered an essential defence against the downstream generation of ROS other than O_2^-, which is even more toxic than superoxide itself. In this function, SOD1 is more efficient than SOD2. Although up-regulated during PRRSV infection in PAMs (Zhang et al., 2009a,b), SOD1 was notably down-regulated during PRRSV infection; further investigation will be required to understand its role. Notably, our finding was consistent with a previous report which indicated that PRRSV infection decreased the production of superoxide anion in PAMs.

The abundance of several proteins involved in immune response, antigen processing and presentation were also altered in this study. Western analysis showed that galectin-1 was down-regulated in PRRSV-infected PAMs and Marc-145 cells as compared with uninfected cells galectins, a lectin family, have been implicated in various immune response processes through binding to host surface glycoproteins. Studies suggest that galectins participate in the immune response, both as immunomodulators and molecules that facilitate pathogen–host cell interactions (Kohatsu et al., 2006). In addition, recent evidence indicates that galectins could facilitate pathogen internalization in phagocytic cells, such as macrophages (Van den Berg et al., 2004). Galectin-1 expression has been reported in thymus and lymphoid parenchymal epithelial cells, endothelial cells, trophoblasts, activated T cells, macrophages, activated B cells, follicular dendritic cells and CD4+CD25+ regulatory T cells (Barrionuevo et al., 2007). Galectin-1 can increase adsorption of X4-utilizing isolates of HIV-1 onto CD4+ T lymphocytes, thus enhancing the overall infection process (Mercier et al., 2008). Of these, the decrease in galectin-1 was confirmed by real-time RT-PCR and Western blotting analysis. These data suggest that the proteins identified in this study may play special roles during PRRSV infection or replication.

5. Conclusion

This study adopted a gel-based proteomic approach to probe the differentially altered proteins in PRRSV-infected PAMs and the Marc-145 cellular proteome. Importantly, the comparative proteomic approach identified 29 altered cellular proteins during PRRSV infection. Interestingly, some of the identified proteins have the ability to regulate apoptosis. Our study facilitates a better understanding of the pathogenic mechanisms of PRRSV infection. Further large-scale studies are necessary to understand the roles of the interesting proteins implicated in PRRSV infection.

Acknowledgment

This study was supported by the Agricultural Research Project in Guangdong Province of China (no. 2008A020100020).

References

Alfonso, P., Rivera, J., Herna'ez, B., Alonso, C., Escribano, J.M., 2004. Identification of cellular proteins modified in response to African swine fever virus infection by proteomics. Proteomics 4, 2037–2046.

Barrionuevo, P., Beigier-Bompadre, M., Ilarregui, J.M., Toscano, M.A., Bianco, G.A., Isturiz, M.A., Rabinovich, G.A., 2007. A novel function for galectin-1 at the crossroad of innate and adaptive immunity: galectin-1 regulates monocyte/macrophage physiology through a nonapoptotic ERK-dependent pathway. J. Immunol. 178, 436–445.

Blackstock, W.P., Weir, M.P., 1999. Proteomics: quantitative and physical mapping of cellular proteins. Trends Biotechnol. 17, 121–127.

Duan, X., Nauwynck, H.J., Pensaert, M.B., 1997. Virus quantification and identification of cellular targets in the lungs and lymphoid tissues of pigs at different time intervals after inoculation with porcine reproductive and respiratory syndrome virus. Vet. Microbiol. 56, 9–19.

Emmott, E., Rodgers, M.A., Macdonald, A., McCrory, S., Ajuh, P., Hiscox, J.A., 2010. Quantitative proteomics using stable isotope labeling with amino acids in cell culture reveals changes in the cytoplasmic, nuclear, and nucleolar proteomes in Vero cells infected with the coronavirus infectious bronchitis virus. Mol. Cell. Proteomics 9, 1920–1936.

Gao, G., Luo, H., 2006. The ubiquitin–proteasome pathway in viral infections. Can. J. Physiol. Pharmacol. 84, 5–14.

Kim, H.S., Kwang, J., Yoon, I.J., Joo, H.S., Frey, M.L., 1993. Enhanced replication of porcine reproductive and respiratory syndrome (PRRS) virus in a homogenous subpopulation of MA-104 cell line. Arch. Virol. 133, 477–483.

Kohatsu, L., Hsu, D.K., Jegalian, A.G., Liu, F.T., Baum, L.G., 2006. Galectin-3 induces death of Candida species expressing specific beta-1,2-linked mannans. J. Immunol. 177, 4718–4726.

Liu, N., Song, W., Wang, P., Lee, K., Chan, W., Chen, H., Cai, Z., 2008. Proteomics analysis of differential expression of cellular proteins in response to avian H9N2 virus infection in human cells. Proteomics 8, 1851–1858.

Manevich, Y., Fisher, A.B., 2005. Peroxiredoxin 6, a 1-Cys peroxiredoxin, functions in antioxidant defense and lung phospholipids metabolism. Free Radic. Biol. Med. 38, 1422–1432.

Mercier, S., St-Pierre, C., Pelletier, I., Ouellet, M., Tremblay, M.J., Sato, S., 2008. Galectin-1 promotes HIV-1 infectivity in macrophages through stabilization of viral adsorption. Virology 371, 121–129.

Nauwynck, H.J., Duan, X., Favoreel, H.W., Van, Oostveldt-P., Pensaert, M.B., 1999. Entry of porcine reproductive and respiratory syndrome virus

into porcine alveolar macrophages via receptor-mediated endocytosis. J. Gen. Virol. 80, 297–305.
Ringrose, J.H., Jeeninga, R.E., Berkhout, B., Speijer, D., 2008. Proteomic studies reveal coordinated changes in T-cell expression patterns upon infection with human immunodeficiency virus type. J. Virol. 82, 4320–4330.
Stefanovic, S., Windsor, M., Nagata, K.-I., Inagaki, M., Wileman, T., 2005. Vimentin rearrangement during African swine fever virus infection involves retrograde transport along microtubules and phosphorylation of vimentin by calcium calmodulin kinase II. J. Virol. 79, 11766–11775.
Schwarz, K.B., 1996. Oxidative stress during viral infection: a review. Free Radic. Biol. Med. 21, 641–649.
Van den Berg, T.K., Honing, H., Franke, N., van Remoortere, A., Schiphorst, W.E., Liu, F.T., Deelder, A.M., Cummings, R.D., Hokke, C.H., van Die, I., 2004. LacdiNAc-glycans constitute a parasite pattern for galectin-3-mediated immune recognition. J. Immunol. 173, 1902–1907.
Wensvoort, G., Terpstra, C., Pol, J.M., ter Laak, E.A., Bloemraad, M., de Kluyver, E.P., Kragten, C., van Buiten, L., den Besten, A., Wagenaar, F., 1991. Mystery swine disease in the Netherlands: the isolation of Lelystad virus. Vet. Q. 13, 121–130.
Wensvoort, G., Kluyver, E.P., Pol, J.M., Wagenaar, F., Moormann, R.J., Hulst, M.M., 1992. Lelystad virus, the cause of porcine epidemic abortion and respiratory syndrome: a review of mystery swine disease research at Lelystad. Vet. Microbiol. 33, 185–193.
Wood, Z.A., Schroder, E., Robin Harris, J., Poole, L.B., 2003. Structure, mechanism and regulation of peroxiredoxins. Trends Biochem. Sci. 28, 32–40.
Yan, J.X., Wait, R., Berkelman, T., Harry, R.A., Westbrook, J.A., Wheeler, C.H., Dunn, M.J., 2000. A modified silver staining protocol for visualization of proteins compatible with matrix-assisted laser desorption/ionization and electrospray ionization-mass spectrometry. Electrophoresis 21, 3666–3672.
Yokota, S., Yokosawa, N., Kubota, T., Okabayashi, T., Arata, S., Fujii, N., 2003. Suppression of thermotolerance in mumps virus-infected cells is caused by lack of HSP27 induction contributed by STAT-1. J. Biol. Chem. 278, 41654–41660.
Zandi, F., Eslami, N., Soheili, M., Fayaz, A., Gholami, A., Vaziri, B., 2009. Proteomics analysis of BHK-21 cells infected with a fixed strain of rabies virus. Proteomics 9, 2399–2407.
Zhang, X., Zhou, J., Wu, Y., Zheng, X., Ma, G., Wang, Z., Jin, Y., He, J., Yan, Y., 2009a. Differential proteome analysis of host cells infected with porcine circovirus type 2. J. Proteome Res. 8, 5111–5119.
Zhang, H., Guo, X., Ge, X., Chen, Y., Sun, Q., Yang, H., 2009b. Changes in the cellular proteins of pulmonary alveolar macrophage infected with porcine reproductive and respiratory syndrome virus by proteomics analysis. J. Proteome Res. 8, 3091–3097.
Zheng, X., Hong, L., Shi, L., Guo, J., Sun, Z., Zhou, J., 2008. Proteomic analysis of host cells infected with infectious bursal disease virus. Mol. Cell. Proteomics 7, 612–615.